

# The Effect of Processing Variables on the Formation and Removal of Bubbles in Rotationally Molded Products

A. G. SPENCE and R. J. CRAWFORD

*School of Mechanical and Process Engineering  
Queen's University  
Belfast BT9 5AH, Northern Ireland*

The rotational molding processing method for plastics is steadily expanding its product range and market areas. However, a drawback of the process has always been the surface pin-holes and internal bubbles that occur in the products because of the inherent nature of the process. In an attempt to alleviate this problem, a program of research has been carried out to investigate the factors that affect the formation of the bubbles and, more importantly, that influence their removal. This paper describes the results of the first stage of this work and covers variables such as the viscosity of the polymer melt, the nature of the pigmentation, the particle size, shape and distribution in the powder feedstock, the mold release agent, the metal used for the mold, the temperature distribution in the mold, etc. It is shown that the mechanisms of bubble formation and removal can be explained and having done this, steps can be taken to ensure that once formed, the bubbles will decrease in size rapidly. This provides significant advantages in terms of reduced cycle time and improved product quality.

## INTRODUCTION

In its most basic form, rotational molding is a method for producing hollow plastic articles. The principle of the process is straightforward. A predetermined charge of cold plastic powder is placed in one half of a cold mold—usually sheet steel or cast aluminum. The mold is then closed and subjected to biaxial rotation in a heated environment, as shown in *Fig. 1*. As the metal mold becomes very hot, the plastic powder tumbling inside the mold starts to melt and coat the surface of the mold. When all the powder has melted, the mold is transferred to a cooled environment. The biaxial rotation continues until the plastic has solidified. At this point the mold is opened and the part is removed. The final product used need not be hollow since finishing operations such as cutting or sawing can be used to make, for example, right and left handed articles (1, 2). Unlike most other molding methods for plastics, rotomolding does not utilize pressure to force the melt into shape, and hence the moldings are essentially stress free.

Polyethylene tends to dominate the market as a rotomolding material due to its high thermal stability and the wide range of grades that have been developed specifically for the process. However, other thermoplastics such as PVC, ABS (acrylonitrile-butadiene-styrene copolymer), polycarbonate, polyester, poly-

amides, and even some thermosets can be rotomolded successfully. In recent years the geometry of molded parts has become even more complex as designers become familiar with the process and take advantage of its potential. A particular feature of rotational molding is its flexibility, both in terms of the shape of the end-product and its size. For example, current products range from ear syringes to 100,000 liter storage tanks. Inserts can be readily molded-in and fine surface detail such as wood grain may be accurately reproduced. Although wall thickness cannot be controlled as precisely as with injection molding, it is possible to get a fairly uniform wall thickness when this is desired. To a large extent this must be done by trial and error at present, but recent developments (3-5) assist with the identification of optimum speed ratios, temperatures, etc. Machine design also has an important role to play in the production of good quality moldings.

It is widely recognized that rotational molding has a number of drawbacks relative to other processing methods for plastics. One of these is the lack of precise control over the condition of the powder/melt inside the mold. Another is the occurrence of bubbles within the melt that may be retained in the solid plastic product and in some cases appear as pit marks on the surface. The former problem has to a large extent been

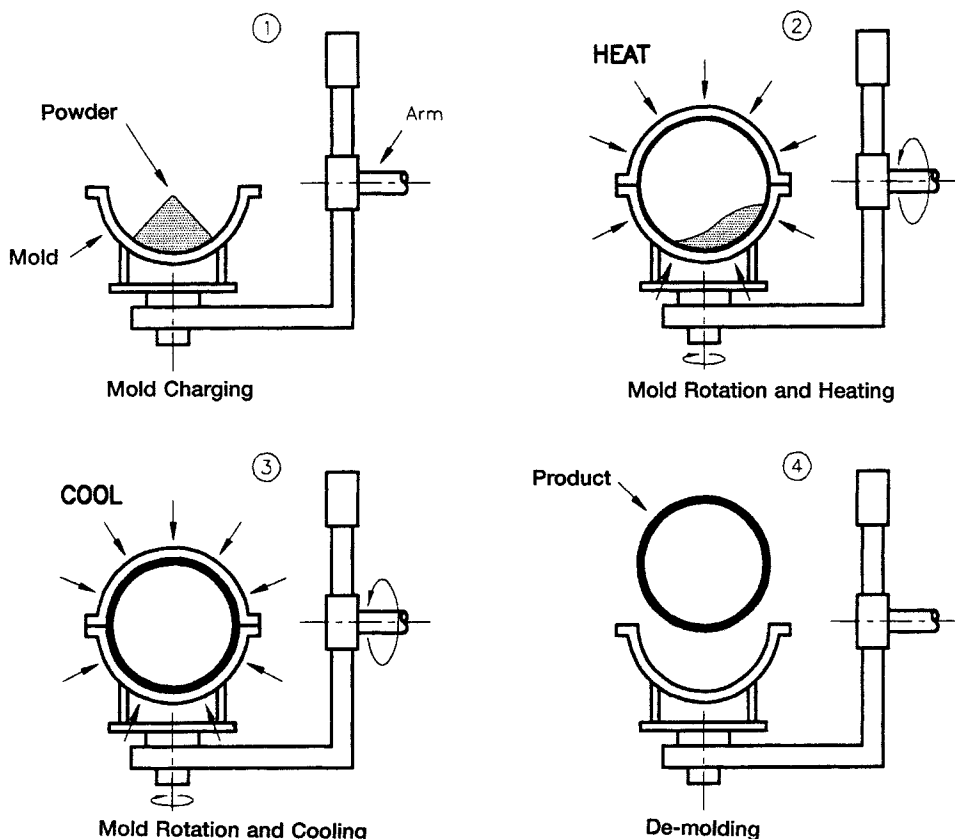


Fig. 1. Principal stages in rotational molding.

overcome by the development of ROTOLOG (5) at Queen's University. This equipment permits the conditions inside the rotating mold to be monitored throughout the molding cycle so that the process can be controlled very precisely. However, the second problem—that of bubble formation and removal—is not well understood and so this program of work was set up to investigate these phenomena. During this work a number of parameters were identified as contributing to the formation and/or removal of bubbles in rotomolded products. These included:

1. Powder—particle shape, size and distribution
2. Viscosity of melt—MFI
3. Additives—(e.g. pigments)
4. Mold surface
5. Temperature
6. Time
7. Atmosphere inside the mold
8. Surface tension
9. Vacuum
10. Pressure.

This paper presents the initial results from the research carried out on bubbles in rotomolded products. These results concentrate specifically on the parameters related to the processing variables available to the rotational molder.

### Bubbles in Rotational Molding

The presence of bubbles in rotationally molded products has been recognized for many years (6, 7).

However, there is a lack of understanding of how bubbles and pores form. In the past it has generally been felt that product quality is at its best when all air pockets have been removed from the material (8). In 1965, the United States Industrial Chemicals Company published a paper on rotational molding of polyethylene powder (6). A number of recommendations were made to solve the problem of bubbles in a molded item. The solutions that were recommended, included raising the oven temperature, increasing the heating cycle, using a material with a high melt flow index or using a material with a lower density.

In that same year, McKenna (7) of Union Carbide explained that bubbles are caused by air entrapment between powder particles. A point was also made about powder particle shape. If the powder particle has irregular, long thin protrusions this will give rise to a low packing density, and hence more bubbles will be trapped in the powder pool. Some mechanical properties of the plastic were quoted, indicating that a void-free part has better low temperature impact strength and a greater elongation to failure, relative to a sample tested with a large distribution of bubbles.

In 1972 Rao and Throne (9) also made reference to particle geometry, suggesting that the most desirable particle shape is cubic with generously rounded corners. They related particle size to the concentration of pores on the surface of the molded part. An additional amount of finer particles in the powder mixture will reduce porosity, improve heat transfer to the plastic, and will help the powder flow by lubricating the move-

ment of the larger particles. Ramazzotti (10) pointed out that larger particles sizes, when used with a high viscosity material, result in poor surface reproduction and a tendency to trap air in the form of bubbles when the part is formed.

Moisture content was recognized by several authors (11-13) as a cause of bubbles and pores in molded parts. Both the quality and surface finish are impaired, and the strength of the product is considerably reduced when hygroscopic raw materials pick up excess moisture in transit and storage. The grinding of these resins greatly increases the surface area that is available for moisture pick-up. The moisture can vaporize during molding and create bubbles and surface pitting of the part. The addition of carbon black pigmentation can also increase the rate at which moisture is picked up (14). The problem of moisture does not apply singularly to polyethylene, but is more widely associated with materials such as polycarbonate, nylon, and ABS. It is recommended that these materials be dried prior to molding. Polycarbonate, in particular, is known to produce moldings with a high proportion of bubbles and pores. It has been suggested (14) that the problem could be alleviated by increasing the internal pressure using nitrogen gas.

With the introduction of crosslinkable grades of polyethylene for rotational molding, bubbles have been identified as being a problem for the molder (15). The size and thickness of the part magnify the bubble problem inherent in molding crosslinked polyolefins. Carrow (16, 17), in his work on high density polyethylene, refers to bubbles caused by decomposition of the crosslinking agent. Surface porosity of the molding can result from the wrong type of release agent and also from small cavities in the wall of the mold.

Brenzinch *et al.* (18) tabulated a "troubleshooting" guide, and suggested solutions for gas entrapment when molding plastisols. These solutions included lowering the plastisol viscosity or the addition of a viscosity depressant. A more detailed investigation of the problem of bubble formation in PVC plastisols was performed by Eileen Harkin-Jones (19). She discovered that the rate of viscosity increase will affect the number of bubbles that form. A rapid rise of viscosity results in the mold wall lifting a greater quantity of material, which can not be supported as the mold rotates. Plastisol therefore drips back into the pool, and so air is trapped. However, with a gradual increase in viscosity, less plastisol is lifted by the mold wall. This results in the plastisol being easier to support and hence, fewer bubbles form.

Howard (3) discussed the problem of bubbles and surface pores that were caused by adding a percentage of regrind material with a virgin polymer. He initially used a material with a high melt flow index (15 g/10 min), which when molded, produced a product without pores or bubbles. He found that a mixture containing 10% of regrind material produced a molding with few bubbles and pores. Further increases in the percentage of reground material produced a product with severe bubbles and surface pores.

## Sintering and Densification

It is apparent from the previous section that a large number of previous workers have referred to the presence of bubbles in rotationally molded products. However, only a few researchers have made a serious attempt at explaining how bubbles are formed and how they are removed.

In an initial attempt at this problem, Rao and Throne (20) drew extensively from the theories of metal sintering and glass densification. It was suggested that the formation of a homogeneous melt from powder particles involves two distinct steps:

1. The particles stick or fuse together at their points of contact. This fusion zone grows until the mass becomes a porous three-dimensional network, with relatively little density change. This is referred to as **sintering**.
2. At some point in the fusion process, the network begins to collapse into the void spaces. These spaces are filled with molten polymer that is drawn into the region by capillary forces. This is referred to as **densification**.

Rao and Throne used this model to explain features such as surface porosity of moldings. They suggested that these occur because the voids in the powder interior, that are formed upon densification, are pushed ahead of the melt front to the free surface. However, the buoyancy, capillary, and hydrodynamic forces that force the interior void away from the mold surface, are not strong enough to overcome the surface tension force required to pull the surface void away from the mold surface and into a bubble. It is concluded therefore, that surface porosity is intrinsic to the process.

Ten years later, Progelhof *et al.* (21) further developed the powder densification theory. Their updated theory suggested that as the powder is heated, the particles become sticky and adhere to each other, and upon further heating, the particles fuse together or densify to form a unitized structure. From observing hot plate experiments, Throne and his associates concluded that as the heating process continues, the solid/melt interface moves upwards, the top of the free surface of the powder drops, and with time the powder completely melts. Throne *et al.* also observed the formation of voids. The voids appeared to be a result of a bound inclusion of the space between individual particles, and the most striking point was the slow movement of voids to the free surface. There appeared to be some coalescence of voids, but with time the voids diminished in size.

Kelly (22) of DuPont Laboratories, Canada, also considered powder densification in an unpublished paper. Kelly suggested that air bubbles are trapped in the polymer during melting, and decrease in diameter as the melt temperature increases. The high viscosity of the melt prevents movement of the bubbles. At a high enough melt temperature, the air in the bubbles begins to dissolve into the polymer. Oxygen has about

twice the solubility of nitrogen in polyethylene. At high temperatures, the oxygen is further depleted by direct oxidation reactions with polyethylene. The depletion of oxygen reduces the bubble diameter. The laws of surface tension dictate that the pressure inside the bubble has to increase as the diameter decreases. The increase in pressure forces the nitrogen to dissolve in the polymer, thus the bubble diameter is further reduced and this chain of events repeats until the bubble disappears. As cycle time increases, the size and quantity of bubbles decrease. At very long cycle times, the molded part will have no bubbles. However, impact strength is low because the polyethylene has oxidized. Kelly also refers to a critical bubble size above which the gases will not dissolve regardless of temperature or time, because the surface tension forces cannot generate enough bubble pressure to help dissolve the gases inside the bubble.

### THEORY OF BUBBLE DYNAMICS

To understand the bubble formation and removal mechanism, it is necessary to understand the process of polymer sintering and densification. Solid particles, when in contact with one another at elevated temperatures, tend to decrease their total surface area by coalescence. This process, called sintering, is usually accompanied by a decrease of the total volume of the powder mass. A decrease in surface area brings about a decrease in surface free energy, thus the surface tension is the predominant force for the coalescence process.

Frenkel (23) was the first person to consider the concept of viscous sintering, and derived an expression for the rate of coalescence of adjacent spheres under the action of surface tension. From the model given in Fig. 2, he developed a theory that predicts the variation of the sintering process with time for two identical spheres. The Frenkel expression takes the form:

$$\frac{x^2}{r} = \frac{3}{2} \left( \frac{\gamma}{\eta} \right) t \quad (1)$$

where:

- $x$  is the neck radius as represented schematically in Fig. 2
- $r$  is the radius of the spheres
- $\gamma$  is the surface tension
- $\eta$  is the viscosity
- $t$  is the time.

This relationship has been confirmed by Kuczynski and Zaplatynsk (24) for the sintering of glass. For the second stage of the sintering process, normally described as densification, these authors were able to derive an equation in the form of:

$$r_o - r = \frac{\gamma t}{2\eta} \quad (2)$$

where:

- $r_o$  is the initial radius of the pore
- $r$  is the reduced radius at time  $t$ .

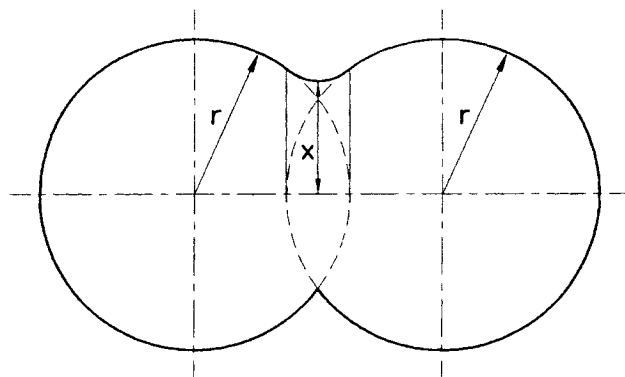


Fig. 2. Model for sintering concept.

This expression was applied successfully to glass ceramic materials, but for polymeric materials Kuczynski *et al.* (25) working with polymethylmethacrylate (PMMA), found that the experimental data conformed to the general expression:

$$\left( \frac{x^2}{r^{1.02}} \right)^n = K(T)t \quad (3)$$

where:

- $K$  is an experimental constant
- $T$  the temperature
- $t$  the sintering time
- $r$  the radius of the PMMA sphere
- $x$  the radius of the interface.

The exponent  $n$  decreases from 5 to  $\sim 0.5$  as the sintering temperature increases from 127° to 207°C.

In 1962, Lontz (26) studied the sintering of polytetrafluoroethylene and suggested that for viscoelastic sintering, the time-dependent interfacial ( $x/r$ ) coalescence should be more properly described as:

$$\frac{x^2}{r} = \frac{3}{2} \left( \frac{\gamma t}{\eta_o(1 - e^{-t/\tau})} \right) \quad (4)$$

where:

- $\eta_o$  represents the initial viscosity
- $\tau$  is an apparent relaxation constant to be assigned from experimental determinations to account for both inherent and stress-induced retardation.

As the sintering proceeds and coalescence and densification occur, the overall heat conduction problem does not remain unaffected. Clearly, the effective thermophysical properties change, influencing the overall temperature distribution, and hence the local sintering problem as well.

Crawford and Scott (27, 28) carried out hot plate tests on powders, using video equipment to record and examine the processes of melting in detail. They based the conditions on earlier measurements made during actual molding trials. The video recording allowed the formation and subsequent dissolution of bubbles to be recorded and modeled. They described the melting

and collapse of the powder as heat is applied from the base as two bulk movements (see Fig. 3). First, the progression of the melt front through the powder mass to the free surface and the collapsing of powder particles into the melt. It is the latter that tends to trap air. A force analysis on a typical bubble shows that the apparent viscosity of molten polyethylene is so large that the buoyancy forces acting on it are insignificant. They also stated that the trapped air will diffuse into the surrounding polymer mass and produced bubble measurements to support this. The initial size of the bubble has a significant effect on the rate at which it dissolves, as the surface area-to-volume ratio is inversely proportional to the diameter. From their work, Crawford and Scott derived a relationship that modeled the removal of gas bubbles from a polymer melt that took the following form:

$$\left(\frac{\phi}{\phi_0}\right)^2 = K_3 - K_2 t \quad (5)$$

where:

- $\phi$  is the diameter of the bubble
- $\phi_0$  is the original diameter of the bubble
- $t$  is time
- $K_2$  and  $K_3$  are constants

Crawford and Xu (29) complemented Scott's earlier work on bubble analysis. They improved upon Scott's model for the removal of bubbles from the melt and found that it was more accurate to say that the following type of relationship applied:

$$\left(\frac{\phi}{\phi_0}\right)^2 = K_5 - K_2 t + K_6 t^2 \quad (6)$$

where:  $K_5$  and  $K_6$  are constants.

This relationship was used to illustrate graphically how the removal of gas bubbles from the polymer melt was influenced by the melt temperature.

### MATERIALS, EQUIPMENT, AND TEST METHODS

During the course of this work a number of different materials were investigated (see Table 1). The mechanism of bubble formation and removal was observed using a Hot Plate technique. During the hot plate test, a 50 g sample of powder was placed on a base plate enclosed by a cylindrical ring complete with a glass viewing port. Thermocouples were positioned at vari-

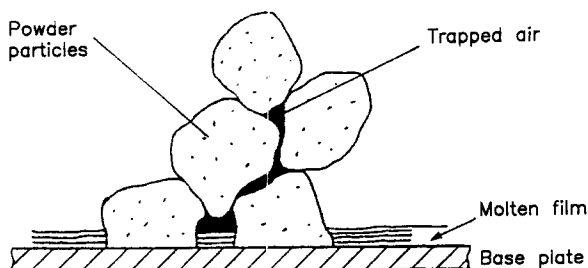


Fig. 3. Bubble formation in a melting powder.

Table 1. Materials Tested in this Study.

Material	Type	Color (Compounded)	MFI (g/10 min)	Density
NCPE 8017	MDPE	Natural	3.2	934
NCPE 8645	MDPE	Natural	8.0	935
MIL 3712	MDPE	Natural	12	937
MIL 3718	MDPE	Natural	18	937
MIL 3725	MDPE	Natural	25	937
NCPE 8113	MDPE	Sky blue	3.2	934
NCPE 8628	MDPE	Black	3.2	935
NCPE 8644	MDPE	Emerald	8.0	935
NCPE 8644	MDPE	Beige	8.0	935
NCPE 8605	MDPE	Black	8.0	935
DuPont 8107	LDPE	Natural	5.0	924
DuPont 8107	LDPE	Black	5.0	924
DSM 2H178	LDPE	Natural	4.5	921
DSM 2H178	LDPE	Black	4.5	921
Enichem 546H	MDPE	Sky blue	4.2	935

ous heights above the base plate to monitor the polymer temperature as it melted. The thermocouples were linked to a PC, which provided continuous temperature profiles of each polymer layer. The images of bubbles as they formed and disappeared were observed by a video camera through the viewing port in the enclosing ring. Each test was recorded on video tape and then recalled at a more convenient time for bubble measurement purposes. Accurate bubble measurement was achieved with the aid of a computer hardware package called VIDIC PC 24.

The system, which operated within Windows, was linked directly to the video recorder. Bubble images were transferred from the video to the PC screen where they were analyzed, or stored as required. Generally two bubbles from each melt were measured, and their sizes recorded in pixels. By video recording an object of known size, a pixel to millimeter scaling factor was established. The size of each bubble could then be determined in millimeters.

The rheological properties of each polyolefin material were measured using the Carri-med CSL 100 Controlled Stress Rheometer. The system was a drive/displacement measuring combination comprised of:

- (a) A microprocessor controlled induction motor drive.
- (b) A minimum friction low inertia air bearing.
- (c) A high resolution digital optical displacement encoder.

A controlled stress was applied to the sample placed between the measuring plates. The resulting strain was measured by the optical displacement encoder and fed to a microcomputer. The microcomputer software then calculated the values of viscosity from the stress-strain data, and a plot of viscosity vs. shear rate was produced.

A Caccia RR 1400A shuttle type machine was used for all molding tests during this work. This machine has an offset arm, capable of carrying molds up to 175 kg with a maximum diameter of 1400 mm. The oven is heated by a gas generated flame, and a circulating fan

provides a uniform oven temperature. The burner capacity is 77,000 kcal/h, which allows a maximum operating temperature of 400°C.

The molds used during these tests were cubic in shape. The mold coded QUB1 mold was a cast aluminum mold, with 260 mm sides  $\times$  10 mm thick and containing a 100 mm cube inverted corner. The mold was split along its centerline with each half having a 3° draft angle. The mold coded QUB2 mold was fabricated from 16 gauge (1.6 mm) mild steel with a reinforced lid. The mold was 300 mm square at the base with 300 mm sides tapered to provide a 330 mm square opening. Standard molding conditions consisted of producing a 3 mm part by setting the oven temperature to 300°C and removing the mold from the oven when its internal air temperature reached 195°C. During molding, the primary rotation was set at 7.8 rpm and the secondary rotation at 5.6 rpm.

Polymer grinding was carried out using the Wedco S-12 pilot 4D grinding system. During the grinding operation, polymer granules passed from the hopper via a vibrating feed tray, into the mill. They were ground between two plates, one of which was rotating at approximately 8000 rpm. During grinding, the plate separation was kept constant, as was the air around the mill. The grinding cycle was repeated with all machine parameters being kept constant. After the second grind, all the large particles were removed using a 600  $\mu$ m sieve.

Thermal images of molds and moldings were obtained using the Agema 880 LWB Thermal Imager. When operating the system, it was important to ensure that the image was in focus, perpendicular to the imager, and that the correct temperature scale was selected. Thermal images of molds were obtained by stopping the mold rotation at the desired moment, attaching a mounting bracket (with imager) to the mold, and obtaining a multi-color pattern of the temperature distribution on the surface being studied.

Surface pores were examined using an electron microscope. However, a more detailed analysis was carried out using a Quantimet 500 image analyzer. The image was used to scan a series of 6 mm square areas of each molded part. The output from the analyzer provided details such as number of pores, largest pore, smallest pore, average pore size, and percentage area of pores. This equipment was also used to measure bubbles contained within the wall of the molded part.

The approximate surface tension of various mold materials was determined using liquids of known surface tension. Liquids ranging from 31 dynes/cm to 69 dynes/cm were used during this test. The surface tension of each mold material was determined by lightly spreading a test solution over a 25-mm-square area. The time taken for the liquid to break into droplets was recorded. If the liquid did not disperse into droplets within two sec, then the test was repeated using the next highest dyne level. If the liquid broke into droplets within two sec, then the test was repeated using the next lowest dyne level. When the

solution held exactly two sec before breaking, then the surface tension of the liquid was equal to the surface tension of the material.

## RESULTS AND DISCUSSION

### Material Characteristics

Initial work in this area set out to identify which polyethylene materials were particularly prone to the formation of internal bubbles and surface pores when rotationally molded. To do this a number of materials, commonly used by the rotational molding industry, were molded under standard conditions. The moldings from these trials were then examined and their tendency to form bubbles is listed in Table 2. From this data, it can be seen that the majority of materials with a melt flow index of 8.0 g/10 min or greater, have no bubbles or pores when rotationally molded under standard conditions. This observation has one exception, and that is, when carbon black pigmentation is present, bubbles and pores still exist. Industrial molders regard materials pigmented with carbon black as "problem" materials, with respect to bubbles. However, carbon black has the advantage of providing excellent ultra-violet stability as well as improving the materials resistance to oxidation. If the inclusion of carbon black prevents the passage of ultra-violet rays through the polymer and oxygen into the polymer, then it may also be capable of preventing the air molecules trapped in bubbles passing out of the polymer. At this stage, it was not clearly understood as to how high MFI materials and carbon black pigmentation affect the formation of bubbles. To obtain a better understanding, the melt characteristics of each polymer were investigated.

### Hot Plate Tests

The hot plate test provided a means by which the formation and removal of bubbles could be observed in natural materials. This apparatus was used during the melt-down of five different polymers with melt flow indices ranging from 3.2 g/10 min to 25 g/10 min.

Table 2. Materials that Molded with Bubbles and Pores.

Material	Type	Color (Compounded)	MFI (g/10 min)	Molded With Bubbles and Pores
NCPE 8017	MDPE	Natural	3.2	Yes
NCPE 8645	MDPE	Natural	8.0	No
MIL 3712	MDPE	Natural	12	No
MIL 3718	MDPE	Natural	18	No
MIL 3725	MDPE	Natural	25	No
NCPE 8113	MDPE	Sky blue	3.2	Yes
NCPE 8628	MDPE	Black	3.2	Yes
NCPE 8644	MDPE	Emerald	8.0	No
NCPE 8644	MDPE	Beige	8.0	No
NCPE 8605	MDPE	Black	8.0	Yes
DuPont 8107	LDPE	Natural	5.0	Yes
DuPont 8107	LDPE	Black	5.0	Yes
DSM 2H178	LDPE	Natural	4.5	Yes
DSM 2H178	LDPE	Black	4.5	Yes

Figure 4 illustrates how the diameters of bubbles, at a similar position in each material, change with increasing melt temperature. Figure 5 shows the rate at which each polymer was heated.

From these experiments it was observed that all materials contain bubbles during the initial melt-down phase. This was due to the encapsulation of air between powder particles as they stick and fuse together. As the melt temperature increased, bubbles were observed to diminish in size until after a period of time, they disappeared completely. It should be noted that the rate at which bubbles disappear increases as the melt flow index of the material increases.

These observations may be explained by the fact that as the MFI of the material decreases, the molecular chain length increases. Longer chain lengths not only mean that the melt is more viscous, but also, that the passage of air molecules through the melt is more difficult. In practical terms this means that during the rotational molding cycle there is simply not enough time for bubbles contained in the 3.2 MFI material to diffuse out of the polymer when it is in its molten stage. However, with higher MFI materials (i.e. shorter chains), air molecules have an easier path to the free surface, and so bubbles have ample time during the rotational molding cycle to diffuse out of the polymer.

The general process of the removal of bubbles from each material is similar, and may be influenced by three factors. First, as the melt temperature increases, this causes the pressure inside the bubble to increase. The laws of surface tension dictate (30) that if the bubble pressure increases, then its radius must decrease by an inversely proportional amount. Second, as the melt temperature increases, the polymer structure breaks down and so bonding becomes weaker, allowing the air molecules an easier passage through the melt. Third, at high temperatures, the oxygen contained within bubbles is further depleted by direct oxidation reactions with the surrounding polymer (31-33). This is visibly evident as the polymer has changed from a natural color to a creamy brown.

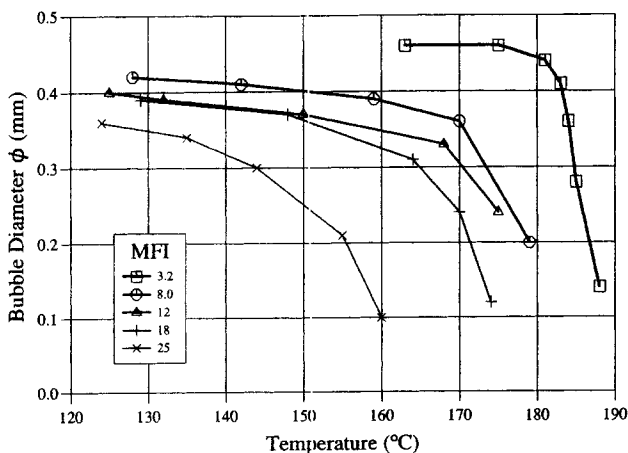


Fig. 4. Hot plate tests.

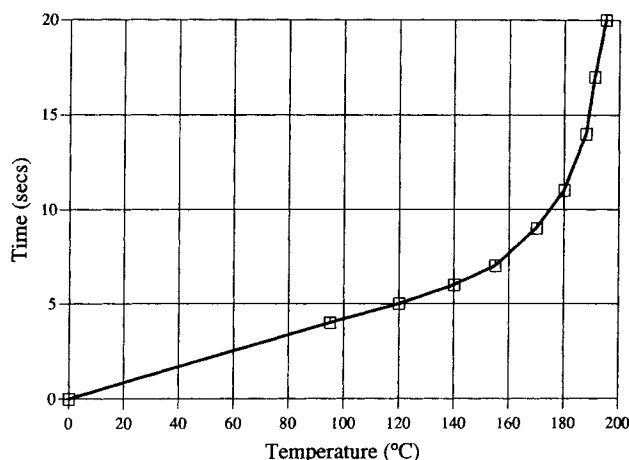


Fig. 5. Heating rates for hot plate tests.

### Melt Rheology

During the rotational molding process the mold is rotated at relatively slow speeds. Unlike other polymer processing techniques this causes low shearing forces between the molten polymer and the mold wall. It was not well known how low shearing rates influence the viscosity of the polymer, which may contain pigmentation such as carbon black. Therefore, it was decided to investigate the viscosity of each polymer over a range of low shear rates to obtain a better understanding of the way in which the melt behaves at various temperatures.

It has been shown by several authors (34-36) that polymer viscosity is influenced by four main factors: shear rate, temperature, molecular weight, and pressure. Prior to testing, the average molecular weight for each material was determined. From Table 3 it can be seen that as the melt flow index increases, the average molecular weight decreases. This can be explained by the fact that the molecular chain length is decreasing. The inclusion of pigmentation does influence the molecular weight, but only by a marginal amount.

Table 3. Average Molecular Weight.

Material	Type	Color (Compounded)	MFI (g/10 min)	Molecular Weight
NCPE 8017	MDPE	Natural	3.2	100,300
NCPE 8645	MDPE	Natural	8.0	80,400
MIL 3712	MDPE	Natural	12	70,000
MIL 3718	MDPE	Natural	18	64,000
MIL 3725	MDPE	Natural	25	59,000
NCPE 8113	MDPE	Sky blue	3.2	97,100
NCPE 8628	MDPE	Black	3.2	99,750
NCPE 8644	MDPE	Emerald	8.0	81,700
NCPE 8644	MDPE	Beige	8.0	81,200
NCPE 8605	MDPE	Black	8.0	77,750
DuPont 8107	LDPE	Natural	5.0	89,550
DuPont 8107	LDPE	Black	5.0	92,100
DSM 2H178	LDPE	Natural	4.5	83,400
DSM 2H178	LDPE	Black	4.5	83,700

Figure 6 illustrates how polymer viscosity, for a range of natural materials, varies with temperature at a constant shear rate of  $0.1 \text{ s}^{-1}$ . As expected, high molecular weight materials correspond to high viscosity values. Polymer temperature has a significant effect on viscosity, particularly for the higher molecular weight materials. It can be seen that the two natural materials (NCPE 8017 and DuPont 8107), which mold with bubbles, are the most viscous. Figure 6 also correlates to the data presented in Fig. 4 and complements what has been previously postulated. It is suggested that air molecules will begin to diffuse out of a natural material when the polymer's viscosity has reached a suitably low level. The upper limit for diffusion to take place appears to be  $\sim 3000$  to  $4000 \text{ Pa.s}$ . Therefore, to accelerate the diffusion process of air bubbles from a high molecular weight material, the viscosity must be reduced, either artificially or otherwise.

One such method that reduces the viscosity of a polymer is to increase its temperature. However, this has a detrimental effect on the polymer structure as it will degrade and accelerate the oxidation process. Another method to reduce the viscosity of a polymer is to increase the rate of shear. Figure 7 illustrates how increasing the shearing rate reduces the polymer viscosity, especially for higher molecular weight materials. Unfortunately this method for reducing the viscosity of the polymer is not suitable for the rotational molding process. Rotational molding is restricted to low shear rates because the mold must rotate slowly, to minimize the inertia forces generated as the relatively heavy mold and contents are rotated.

The effect of compounded pigmentation was also investigated using the rheometer equipment. Figures 8 and 9 illustrate the significant difference in viscosity for the DuPont and DSM materials in natural form, compared to when carbon black pigmentation was added. Figure 9 also highlights that as the shearing rate tends towards zero (as is the case in the rotational molding process), the inclusion of carbon black causes a rapid increase in viscosity. All of these factors suggest that the inclusion of carbon black mole-

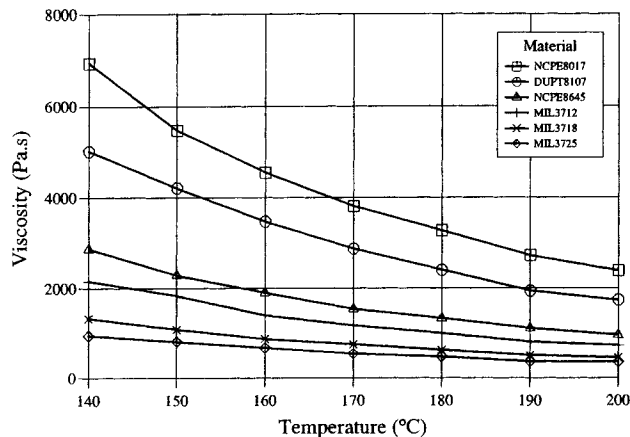


Fig. 6. Viscosity profiles for natural materials at a  $0.1 \text{ s}^{-1}$  shearing rate.

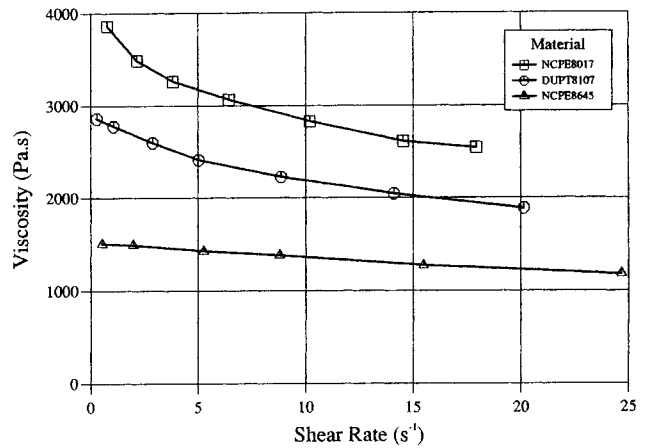


Fig. 7. Viscosity profiles for natural materials at  $190^\circ\text{C}$ .

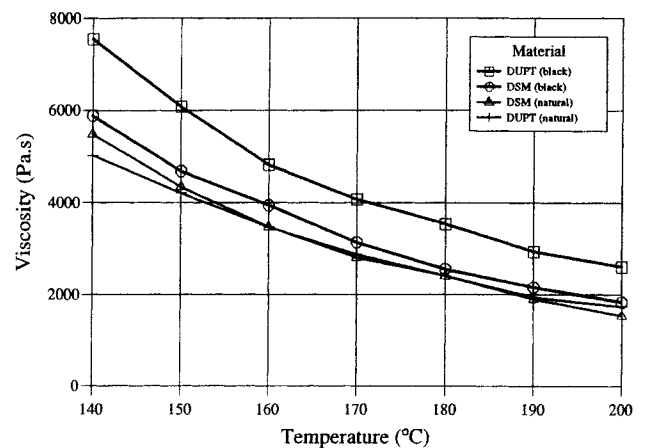


Fig. 8. Viscosity profiles for DSM and DuPont materials at a  $0.1 \text{ s}^{-1}$  shearing rate.

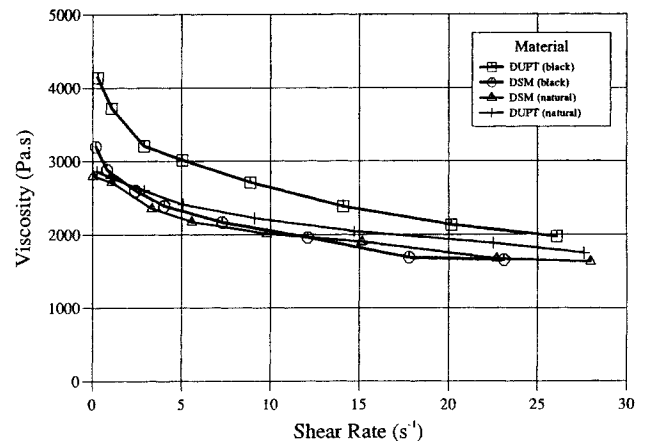


Fig. 9. Viscosity profiles for DSM and DuPont material at  $190^\circ\text{C}$ .

cules restrict the movement of the polymer chains, and so increase viscosity. This may also be related to the fact that the air bubbles find it more difficult to diffuse out of carbon black materials. It is suggested that carbon black molecules obstruct and inhibit the passage of air molecules through the polymer melt.

### Powder Characteristics

The quality of a rotationally molded polyethylene part depends not only on the physical properties of the resin used, but also on the characteristics of the powder, such as its shape, size, and particle uniformity. It has been suggested previously (21) that bubbles that form in rotationally molded parts appear to be a result of air trapped between individual powder particles. Particle shape and size appear to govern the extent of bubbles and pores. It was suggested (7) that long thin powder particles tended to trap more air bubbles in the melt. To achieve optimum flow around the mold, the most desirable particle geometry is a cube with generously rounded corners (9). However, heat transfer during the rotational molding cycle is improved by decreasing the particle size, which in turn increases grinding costs. It was also suggested (37) that surface porosity was particularly affected by the concentration of fine particles. Therefore, it is reasonable to suggest that powder characteristics such as particle shape, size and size distribution will affect the formation of bubbles, and surface pores in particular.

Initial work on the effects of particle size distribution was performed using a black material, NCPE 8628 (MFI 3.2 g/10 min). This material was supplied by Neste Chemicals with two different sizes of grind: a quantity of fine particles (>300  $\mu\text{m}$ ) and a quantity of coarse particles (300 to 500  $\mu\text{m}$ ). The two different grinds were investigated by rotationally molding various percentage mixtures of fine and coarse particles. After molding, the surface porosity of each molded part was investigated. Similar side sections from each molding were observed using the Quantinet 500 image analyzer. The analyzer was used to scan fifteen individual areas that were 6 mm square in size. From these scans, the system software provided information such as the quantity of bubbles, the average bubble size and the percentage area with bubbles. Table 4 lists the results from the fifteen individual scans, for eleven different percentage mixtures.

These results are best analyzed with the aid of a series of graphs. Figure 10 shows the effect of particle size on the average and median pore size. The general observation from this graph is that, as the percentage of fine particles increases, the average pore size and

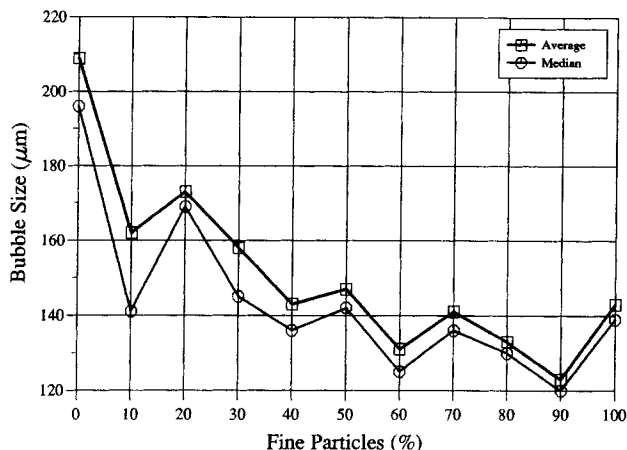


Fig. 10. Effect of particle size on the average and median pore size.

median pore size decrease. This can be explained by the fact that finer particles trap smaller pockets of air, which results in smaller pores. However, it can also be observed from Fig. 10 that the most significant change in the average pore size and median pore size occurs when between 0 and 10% fine particles were used. It is suggested that this is because of the sieving action that takes place during rotational molding. As the powder tumbles inside the mold, the fine particles tend to be sieved to the mold surface. The finer particle therefore melt first against the mold. If this is the case, then the inclusion of more fine particles will have less of an effect on the size of the surface pores, but will increasingly influence the size of bubbles contained in the wall of the part.

Another interesting observation can be seen in Fig. 11, when between 30% and 40% of fine particles were used, the maximum size of pore decreased suddenly. When 40% to 100% of fine particles were used, the maximum size of surface pore changed very little. There seems to be no obvious explanation for this observation. It appears that an optimum level of 40% of fine particles will be equally as efficient as 100% of fine particles at restricting the maximum size of surface pore. The final observation made from the surface pore analysis relates to the percentage of the surface

Table 4. Analysis of Surface Pores for NCPE 8628.

Particle Size		Number of Pores	Maximum Size ( $\mu\text{m}$ )	Average Size ( $\mu\text{m}$ )	Median ( $\mu\text{m}$ )	Porous Area (%)
Fine	Coarse					
0	100%	682	624	209	196	8.4
10%	90%	1066	636	162	141	8.7
20%	80%	883	594	173	169	7.6
30%	70%	1078	587	158	145	7.2
40%	60%	1444	412	143	136	7.1
50%	50%	966	419	147	142	5.5
60%	40%	1389	407	131	125	6.4
70%	30%	1056	379	141	136	5.4
80%	20%	1254	388	133	130	5.8
90%	10%	1505	384	123	120	6.3
100%	0%	1233	355	143	139	6.1

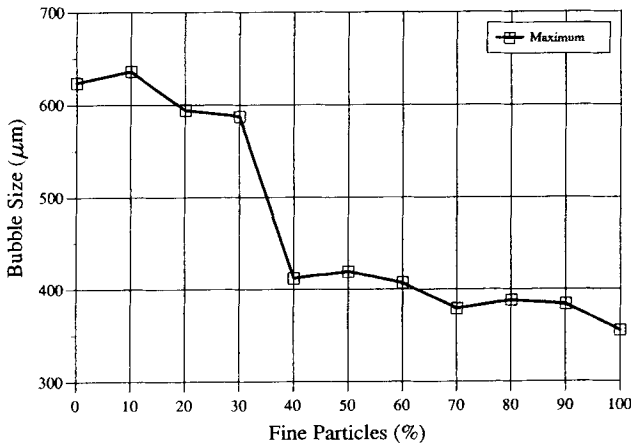


Fig. 11. Effect of particle size on the maximum size of pore.

of the molding that contained pores. Figure 12 illustrates how the percentage of area that contained pores decreased as the percentage of fine particles increased. The general conclusion appears to be that finer particles produce more pores, which are smaller in size, and cover a smaller surface area.

From this work it was decided that a more detailed analysis of the particle shape, size, and size distribution was required to obtain a better understanding of how powder characteristics affect surface porosity. To achieve this, polymer was ground from granules into powder, and the grinding mill parameters varied to obtain different particle shapes, sizes, and size distributions. This work was performed using a Wedco SE-12 pilot 4d grinding system. During grinding, four parameters were varied. First, two types of black polyethylene granules were used, Neste NCPE 8628 and DSM Stamylex 2H 178. Black pigmented materials were used throughout this section as they had been shown in a previous section to produce parts with surface pores and bubbles. Second, the number of teeth on the cutting plates were varied from 240 to 480 teeth. Third, the separation between the cutting plates was varied from 400  $\mu\text{m}$  to 600  $\mu\text{m}$ . Finally, the air temperature around the plates was varied from 30°C

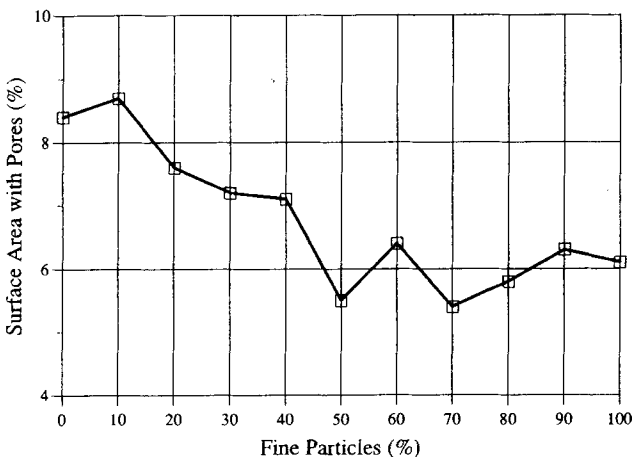


Fig. 12. Effect of particle size on the percentage area of pores.

to 90°C. We hoped that by varying these parameters, the desired effect on powder characteristics would be achieved.

Following polymer grinding, the characteristics of each powder were investigated. It was found that the general effect of increasing the gap size between the cutting blades was an increase in the average particle size. Also, large gap sizes tend to produce more elongated particle shapes, as the particles have more freedom to rotate and hence avoid the shearing action of the cutting teeth. The effect of increasing the number of cutting teeth on the wheel was shown to decrease the average particle size distribution. The decrease in particle size distribution was as expected, as more cutting teeth will shear the powder to a greater extent as it passes between the grinding wheels. Lower grinding temperatures (30°C to 40°C) were found to produce a higher proportion of particles with tails. This phenomenon is due to rapid changes in the polymer temperature caused by coolant circulating through the grinding wheels, which is necessary for this low temperature grind. Tails on powder particles are undesirable as they prevent the particles packing closely together during molding and also inhibit powder flow.

Rotational molding with powders produced from a variety of different grinding configurations highlighted what had been previously suggested. Moldings produced from finer grinds contained more bubbles, which tended to be physically smaller, and also cover a smaller percentage of the external surface of the product. Unfortunately, it would appear the no ideal powder characteristics can be defined so as to prevent bubbles and pores from forming.

### Processing Conditions

Processing conditions refer to areas such as the mold material, oven temperature, heating cycle, cooling cycle, etc. It has been suggested (6) that variations of these parameters may result in parts without bubbles or pores. Therefore it was decided to investigate some of the conditions associated with the rotational molding process.

### Cycle Time

From initial observations of various materials using the hot plate test, it was apparent that bubbles will diffuse out of the material, provided they have enough time to do so. Therefore, during rotational molding, if the period that the polymer is in its molten state can be increased (without increasing the peak internal air temperature), then bubbles have more time to diffuse. Increasing the cycle time without increasing the peak air temperature can be achieved by two methods, either by reducing the oven temperature during molding or by changing the mold material/thickness. The latter of these two methods was used to investigate the effects of cycle time.

Two molds, QUB1 (10 mm aluminum) and QUB2 (1.6 mm mild steel) were used in conjunction with Enichem 546H (MFI 4.2 g/10 mins) to demonstrate

the effect of cycle time. In each case, the Enichem material was molded using the same peak internal air temperature. These trials showed that the mild steel mold, produced moldings with bubbles and pores while the aluminum mold did not.

The reason for this transformation in surface texture becomes apparent after analyzing the Rotolog trace for each molded material (Figs. 13 and 14). The removal of bubbles and pores is not related to the mold material. Bubbles are removed because the polymer is in its molten state for almost twice as long in the aluminum mold, than it is in the steel mold. This can be calculated as the amount of time the internal air trace, for each mold, dwells above the 120°C temperature line. For the aluminum mold this is ~18 min, whereas for the mild steel mold, only 9 min. Therefore, the mold material and mold wall thickness will determine how long the polymer remains in its molten state. This observation addresses one of the myths associated with rotational molding. Industrial molders refer to some molds being more susceptible than others to producing parts with bubbles and pores while using the same material. It is suggested that each mold has an individual thumb print represented by its Rotolog trace. Molds may or may not produce bubbles and pores simply as a result of the amount of time the polymer remains in the molten state during the rotational molding cycle.

**Peak Melt Temperature**

Oven temperature, like cycle time, has been identified (6) as a processing parameter capable of influencing the existence of bubbles. Increasing the oven temperature causes the polymer melt temperature inside the mold to rise accordingly. A series of moldings using NCPE 8605 were carried out to investigate how the peak melt temperature affected bubbles and pores.

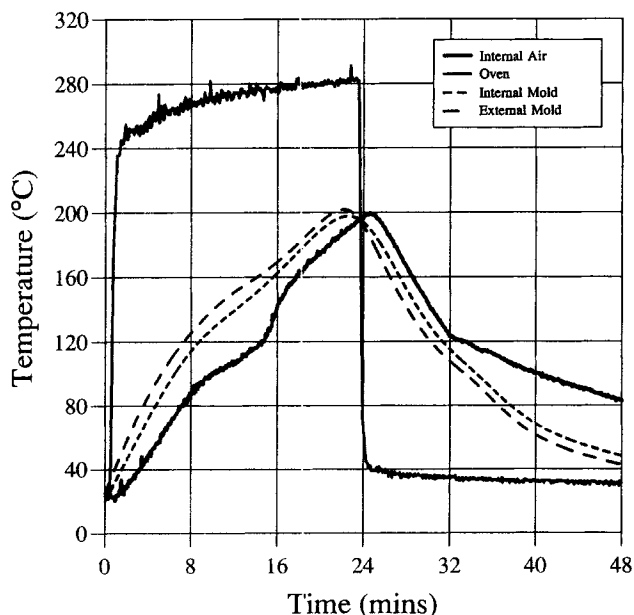


Fig. 13. Rotolog trace for QUB1 aluminum mold.

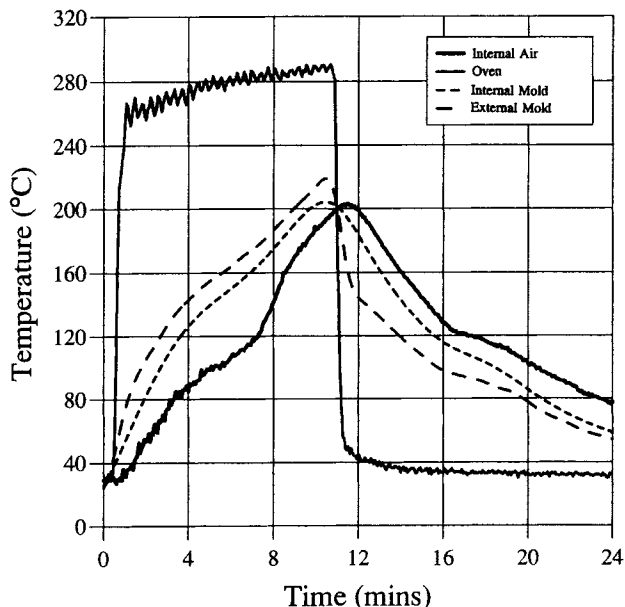


Fig. 14. Rotolog trace for QUB2 mild steel mold.

Five moldings, using the QUB2 mold, were removed from the oven at various peak internal air temperatures. The peak air temperature, which corresponds to the melt temperature, ranged from 125°C to 250°C, when the molded part contained no bubbles. Figure 15 illustrates the Rotolog curves for each molding superimposed on one graph. Increasing the melt temperature has a three fold effect on bubbles. First, higher melt temperatures reduce the viscosity of the polymer making it easier for bubbles to diffuse. Second, higher melt temperatures mean that the polymer will be in its molten state for a longer period of time, again allowing bubbles more time to diffuse. Third, increasing the

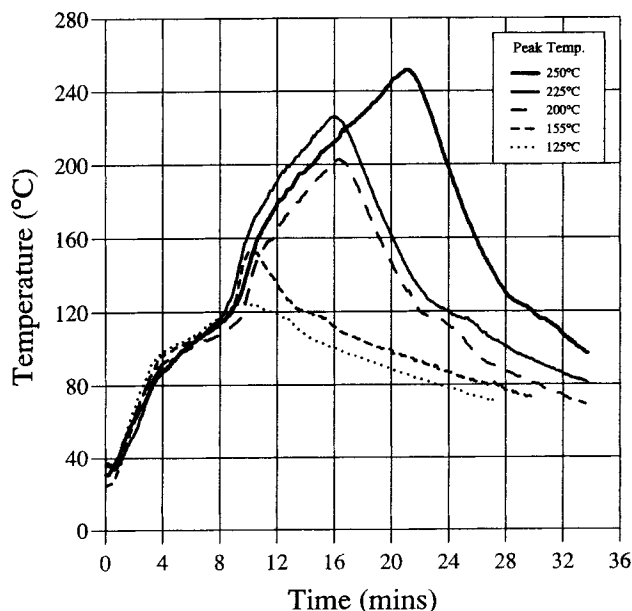


Fig. 15. Rotolog traces for NCPE 8605 for various peak internal air temperatures.

melt temperature, increases the pressure inside the bubble. This results in a reduction in bubble diameter because of surface tension forces.

Examination of the moldings showed that the surface pores only begin to diminish in size at a peak temperature of 225°C, and finally disappear at 250°C. Increasing the temperature of the polymer melt has been shown to be a possible solution to the bubble problem. However, this method of removing bubbles has two major drawbacks. Increasing the melt temperature causes the cycle time to increase, and so productivity drops. The second drawback becomes more apparent when the mechanical properties of the molded parts are investigated. It was found that the impact strength of the molding was particularly affected. Figure 16 illustrates the variation in energies required to break samples molded for different peak temperatures. Brittle fracture was experienced for the two extreme temperatures. This was because the powder particles had not fully formed into a homogenous melt at 125°C. The molding had a rough inner surface, and proved to be very weak. At 250°C the polymer had completely melted with very smooth inner and outer surfaces. However, the polymer has degraded because of oxidation, particularly at the inner surface. This brittle, low strength region acts as a crack initiation zone. Although tensile and flexural strengths were acceptable, the part was extremely fragile at low temperatures (-20°C).

The impact energy graphs also highlight the optimum peak internal air temperature for this material. A peak temperature of ~200°C appears to give maximum impact strength. If the temperature is lower than 200°C then the polymer has not properly consolidated together, and if it is greater than 200°C, the polymer begins to degrade and oxidize. Therefore, bubbles and pores can be removed from rotationally molded products by over-heating the polymer. It should be noted, however, that this takes place at a cost to productivity and some mechanical properties.

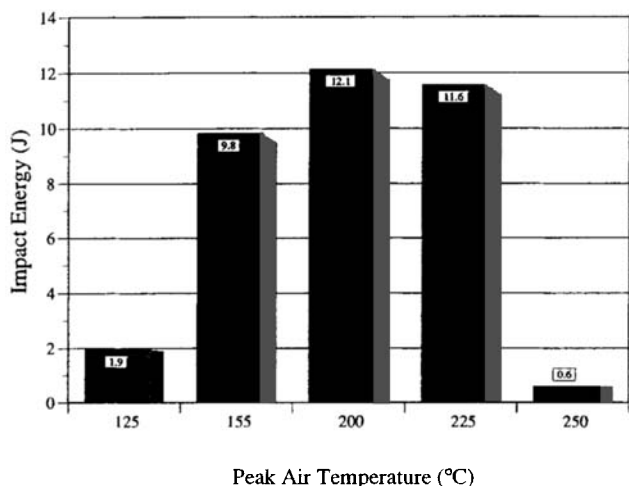


Fig. 16. Impact energy for NCPE 8605 removed from the oven at various peak internal air temperatures (3-mm-thick samples).

### Moisture

Moisture content was recognized by several authors as a possible cause of bubbles and pores in molded parts (11-13). Carbon black pigmentation was also recognized (14) as being hygroscopic, increasing the rate at which moisture is absorbed. To investigate this area, NCPE 8605 (a carbon black pigmented material) was used. The material was first molded in the normal fashion. Then the material was pre-dried to 70°C for one week in a vacuum oven and rotationally molded. Finally, the material was predried to 105°C for one week in the vacuum oven and then molded. The resulting moldings showed no differences. All moldings had a high degree of surface porosity together with bubbles in the wall section. It is suggested that predrying of carbon black pigmented polyethylene materials will not improve the bubble problem. However, predrying may have an effect on other materials such as nylons.

### Cycle Efficiency

The rotational molding cycle is extremely long in relation to other plastics processing techniques. This is necessary to melt, form the shape of the mold, and attain optimum mechanical properties. Also, there is a greater opportunity for bubbles and pores to diffuse out of the polymer, if the heating cycle is long. Therefore, it was decided to investigate if a material with better flow characteristics could be removed from the oven at a lower temperature without any loss of properties. This would help make the rotational molding process more efficient as cycle time would be reduced.

The obvious material to use for these experiments was the material with the highest melt flow index—MIL 3725 (MFI 25 g/10 min). This material was previously shown to mold without bubbles or pores for normal conditions, with a peak internal air temperature of 200°C. A series of moldings were carried out using this material. Five moldings using the QUB2 mold, were removed from the oven at various peak air temperatures. The temperatures ranged from 120°C to 200°C. Figure 17 illustrates the Rotolog curves for all the moldings superimposed on one graph.

From the moldings, a peak internal air temperature of 150°C produced a product without bubbles or pores. The low viscosity of this polymer allowed air molecules an easy passage through the material even at relatively low temperatures. However, at 120°C the molded parts showed poor fusion of the inner surface together with surface pores on the outer surface. The impact strength illustrated in Fig. 18 confirms that the part has not properly fused together at 120°C. Therefore, the excellent flow properties of MIL 3725 allow it to be removed from the oven at 150°C without any significant loss of properties. This can improve cycle efficiency by as much as 25% and still produce a part without bubbles or pores.

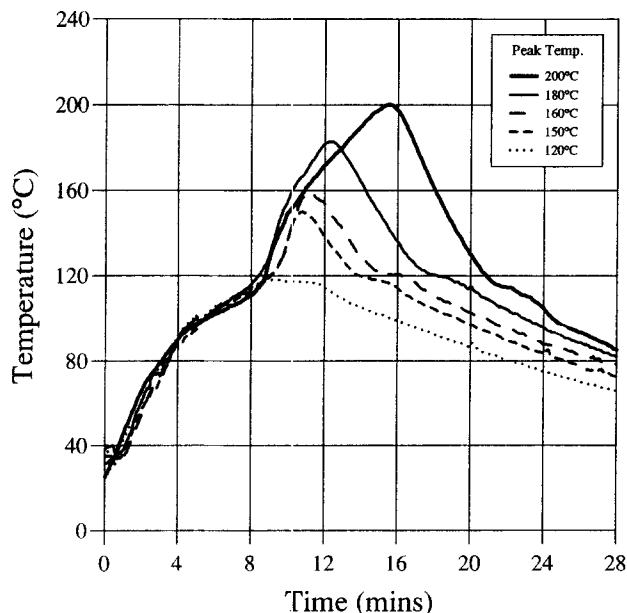


Fig. 17. Rotolog traces for MIL 3725 for various peak internal air temperatures.

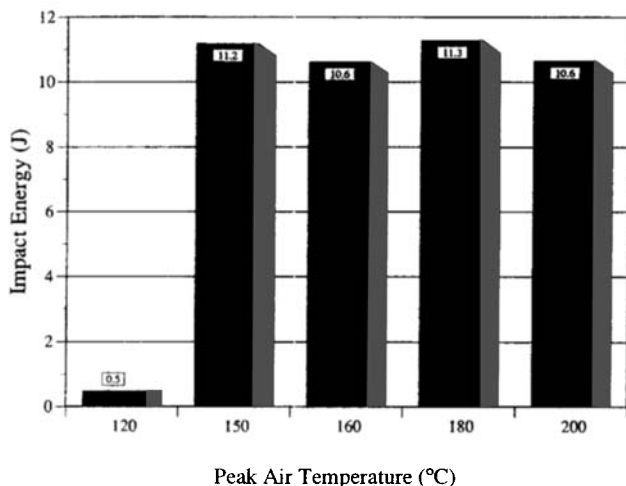


Fig. 18. Impact energy for MIL 3725 removed from the oven at various peak internal air temperatures (3-mm-thick samples).

### Mold Considerations

The quality of any rotationally molded item is governed principally by the quality of the mold used. The mold material, and particularly its internal surface finish are two of the most important factors that influence the appearance of a product. Typically, molds are made from mild steel, stainless steel, cast aluminum or electroformed nickel/copper. The choice of mold material depends on the particular application, the number of molds required, and the surface finish necessary. Another important factor is the type of release agent that is used. Release agent is necessary to aid part removal. However, its effect on the surface of the product has never been investigated.

### Mold Surface Finish

The effect of the surface finish of the mold on the surface porosity of the molded product was investigated using aluminum and mild steel. These two materials were polished to various degrees from their virgin state and then investigated using the hot plate test. Each test consisted of heating 40 g of NCPE 8605, a black polymer with MFI 8.0 g/10 min, on 80 mm square sections of mold material. Heating was terminated when the polymer/melt interface reached 200°C. Examination of the moldings showed that the degree of mold surface finish had little or no effect on the surface porosity of the molded product. In particular, these tests highlighted that there were no advantages in highly polishing a mold, in terms of the surface porosity of the product. However, there would be an improvement in the quality of the product.

### Mold Material

The effect of six different mold materials on the surface porosity of the molded product was investigated using the hot plate test. The materials used included mild steel, stainless steel (mirror finish), aluminum, mild steel chrome plated, brass (mirror finish), and copper. Each hot plate test consisted of melting 40 g of NCPE 8628 (a black polyethylene, MFI 3.2 g/10 min) on 80 mm square sections of material. The hot plate was pre-heated to 300°C and the metal sections removed when the polymer/metal interface reached 200°C. During the hot plate tests, the effect of each material was investigated both with and without the application of a release agent (Mono-coat E 194).

From the tests it was found that the surface porosity experienced for each material with a release agent were quite similar, showing a high density of pores. However, when no release agent was present, with the exception of copper, the surface porosity experienced for each material was significantly reduced. Figures 19 and 20 illustrate how the surface porosity produced by mild steel is influenced by the application of a release agent. The difference in surface porosity ex-

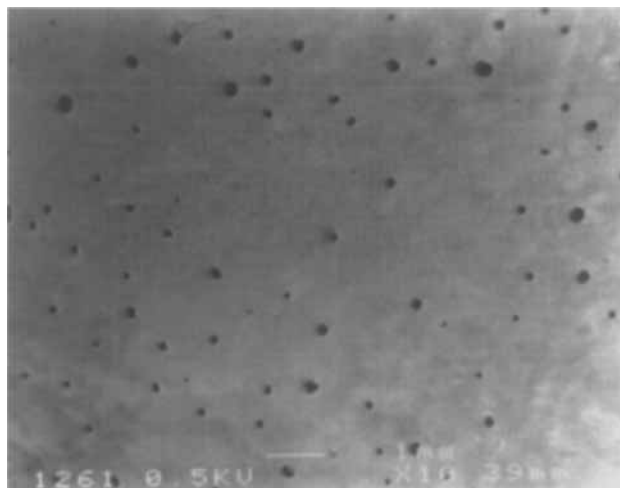


Fig. 19. Mild steel without release agent (magnification  $\times 10$ ).

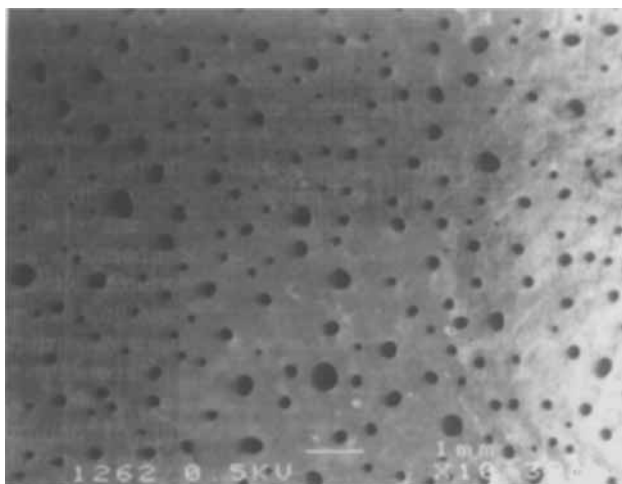


Fig. 20. Mild steel with release agent (magnification  $\times 10$ ).

performed can be explained by the laws of surface tension.

The probability of the molten polymer wetting the surface of the mold depends on the order of surface energies of each of the combining surfaces. If the surface energy of the mold is greater than the surface energy of the molten polymer, then the polymer will wet, and be attracted to the mold. If the surface energy of the mold is less than that of the liquid polymer then the opposite is true. Actual values of surface tension for polyolefins lie in the region of 20 to 50 dynes/c (38), whereas for metals, the values are much greater (39) (typically 100's dynes/c). Therefore, the polymer should, in theory, wet and spread evenly over the surface of the mold.

This theory suggests that the metal sections without release agent, should produce surfaces without pores. However, this is obviously not the case. It is suggested that this is because an oxidation layer has formed on the surface of the metal, which reduces its apparent surface energy/tension. During the hot plate test the oxidation process is greatly accelerated because of the elevated temperature involved (40).

Measurement of the surface tension of each metal section showed that oxidation had taken place. Table 5 lists the experimentally measured surface tension for each metal, with no release agent applied. These values were found to be significantly less than "known" surface tension values for the metals (39). It

has been shown in Fig. 19 that when no release agent was present the surface porosity of the part was greatly reduced. However, the elimination of release agent has a major drawback in that the polymer would adhere to the surface of the mold. Clearly, this would be unacceptable to the rotational molding industry since it would mean that part removal from the mold would become difficult or impossible and the surface of the part would be tarnished.

When each metal section was coated with release agent, the surface porosity experienced was similar, with the exception of copper. These observations again relate to the laws of surface tension. The application of a release agent to a metal surface (which has also been oxidized to some degree) forms an interface between the polymer and the metal. The attractive force that causes the polymer to wet and spread over the surface of the metal is no longer given by the surface tension of the metal, but by the surface tension of the release agent interface. This has a detrimental effect on surface porosity as the very purpose of a release agent is to reduce the bond between the polymer and the mold, to aid part removal.

Measurement of the surface tension for each metal section confirmed how the application of release agent reduced the apparent surface tension of the metal. The data listed in Table 5 highlights the fact that the metal sections with release agent, which produced similar degrees of surface porosity, also had similar surface tensions. The data also shows that the surface tension of copper, both with and without release agent, did not change. However, it is not known why the application of release agent did not reduce the surface tension of the copper plate. It would appear, that for whatever reason, the release agent did not adhere to the copper surface.

#### Mold Release Agent

There are many different types of mold release agent commonly used in the rotational molding industry. The effects of six such release agents on the surface porosity of the molded product was investigated using the hot plate test. The release agents used included Marbocote 75 CEE, Frekote 700 NC, Chemlease 40, Mono-coat E193, Mono-coat E194, and Mono-coat E202. Each hot plate test consisted of melting 40 g of NCPE 8628 (a black polyethylene, MFI 3.2 g/10 min) on a 80 mm square  $\times$  1.2 mm thick mild steel plate pre-coated with a release agent. The application of the release agents to the mild steel plates was conducted in accordance with the manufacturer's recommended procedure. During the tests, the hot plate was pre-heated to 300°C and the metal plates removed when the polymer-metal interface reached 200°C.

From the tests it was found that the surface porosity experienced for each release agent is quite similar. This is not surprising since all the release agents are used in the rotational molding industry for the same purpose, that is, to prevent the polymer adhering to the mold. It was found that the similar effect of each

Table 5. Surface Tension Data.

Material	Surface Tension (dynes/cm)		
	Without Release Agent	With Release Agent	"Known" Value
Mild steel	69	31	—
Stainless steel	50	>31	—
Aluminum	50	>31	860
Mild steel chrome plated	50	>31	1590
Brass	40	>31	—
Copper	69	69	1285

release agent correlated to the surface tension measured for each mild steel plate coated with release agent. In general, the surface tension of the release agent interface is similar for each release agent (see Table 6). This is in agreement with the resulting surface porosity experienced.

It would appear that no "ideal" release agent exists that can provide acceptable non-stick characteristics and also reduce the surface porosity of the molded product. By their very nature, release agents invariably increase surface porosity, as they reduce the force that attracts the polymer to the mold.

#### Mold "Hot Spots"

Rotational molders have observed that some molds produce parts that contain areas with no surface pores, while other areas of the same molding have surface pores. The industry refers to this observation as being due to "hot spots" or areas of the mold that conduct more heat.

To investigate this further, a thermal imager was used in conjunction with a Neste material, NCPE 8113 (sky blue, MFI 3.2 g/10 min), and an aluminum mold (similar to QUB2), which incorporated wall sections of different thickness (3, 6, 9, and 12 mm), to provide areas that varied in temperature. During rotational molding trials, the camera was used to provide a thermal image of the mold when it emerged from the oven. The internal air temperature of the mold was used as a reference, as a series of images were obtained for each mold face.

From the thermal image analysis it was found that the greatest temperature difference occurred, not surprisingly, when comparing the 3 mm wall to the 12 mm wall. A series of thermal images for each face showed that the thermal profile for the 3 mm wall differs significantly from that for the 12 mm wall. The main difference between the two faces is that the 3 mm wall tends to cool initially from the center out, whereas the 12 mm wall tends to be the opposite. This observation can be related to the wall thickness of each mold face and to the thickness of the adjoining walls. The 3 mm face is joined at its left hand side by the 12 mm wall, at its right hand side by the 6 mm wall, and at its base by a 6 mm section. Hence, the cooling of the 3 mm face is influenced by the surrounding heat sinks and appears to cool at the center first. On the other hand, the 12 mm face is joined by thinner sections that cool at a faster rate.

Table 6. Effect of Six Release Agents on the Surface Tension of Mild Steel.

Release Agent	Surface Tension (dynes/cm)
Marbocote 75 CEE	31
Frekote 700 NC	31
Chemlease 40	31
Mono-coat E193	35
Mono-coat E194	35
Mono-coat E202	35

A Rotolog trace (Fig. 21) illustrated that not only did the 3 mm face cool at a faster rate, but it also heated up at a faster rate, and to a higher temperature. The Rotolog temperature profiles for the two walls were given by a thermocouple welded to the center of the internal side of each wall. From the Rotolog trace it can be seen that after only 7.5 min the internal face of the 3 mm wall had reached a temperature (120°C) at which the polymer would begin to adhere to it. This did not happen to the 12 mm wall until ~11 min had past. The resulting wall sections of the molding were thicker, relative to the 3 mm wall of the mold. The thickness of the molding ranged from 3.3 mm to 4.1 mm opposite the 3 mm mold wall, as opposed to 1.6 mm to 2.4 mm, produced by the 12 mm mold wall. The Rotolog profile also highlighted the fact that the temperature of the internal surface of the 3 mm wall peaked at a much higher temperature (207°C) than the temperature of the 12 mm wall (188°C).

The combination of the polymer being in its molten state for longer, and being subjected to a higher temperature by the 3 mm wall, significantly influenced the surface porosity of the part. Figures 22 and 23 illustrate typical surface porosity for the 3 mm and 12 mm mold faces (magnification  $\times 10$ ). From the micrographs it can be seen that the increase in mold thickness causes the size and density of surface pores to increase. The mold thickness governs the temperature of the polymer at each mold face during the molding cycle. As the mold thickness decreases, the polymer is subjected to higher temperatures for longer periods of time. This gives the bubbles and pores more time to diffuse through a less viscous melt. Therefore it can be seen that variations in mold thickness, or variations in the thermal conductivity of specific areas of the mold, will lead to hot or cold spots and this is likely to

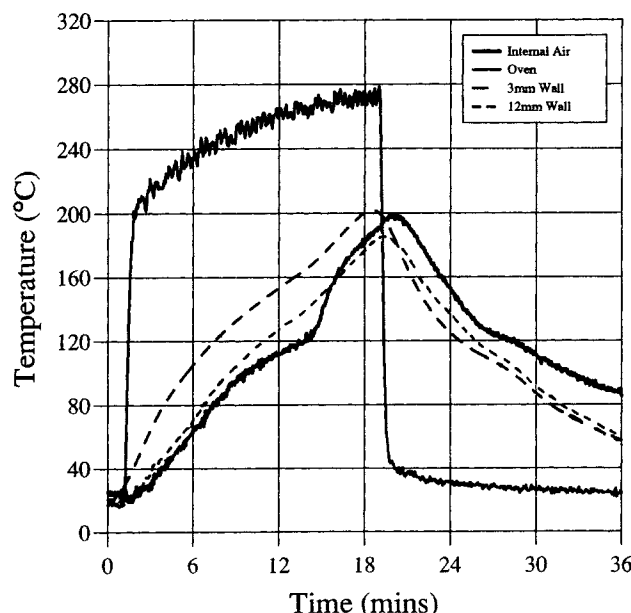


Fig. 21. Rotolog traces for aluminum mold with different wall thickness.

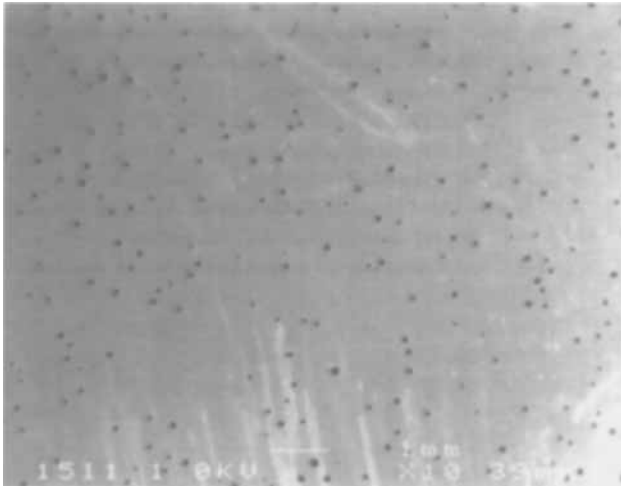


Fig. 22. Surface porosity produced by 3 mm wall (magnification  $\times 10$ ).

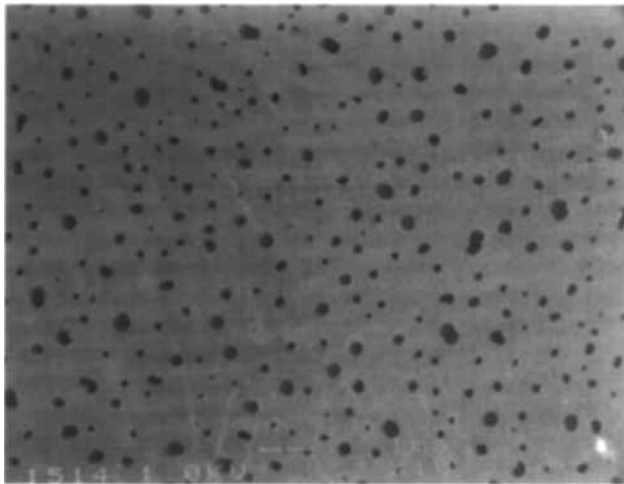


Fig. 23. Surface porosity produced by 12 mm wall (magnification  $\times 10$ ).

result in variations in the surface porosity of the molded part.

### CONCLUSIONS

As a result of this research, the following conclusions may be drawn:

1. Bubbles form because of the encapsulation of air pockets between powder particles as they melt and fuse together. This is true for all materials during the rotational molding process.
2. During the rotational molding process, as the polymer temperature increases, some natural materials allow bubbles that have formed in the melt to slowly diminish in size and finally disappear. The likelihood of this happening has been shown to depend primarily on the viscosity of the polymer used. In general, lower viscosity materials (high MFI materials) allow air bubbles to diffuse more easily.

3. With the exception of carbon black, the inclusion of compounded pigmentation does not affect the rate at which air bubbles diffuse out of the polymer melt. However, the inclusion of carbon black pigmentation was shown to increase the viscosity of the material, and also inhibit the diffusion of air bubbles out of the polymer.
4. The shape, size, and particle size distribution of powder particles used during rotational molding have been shown to influence the size and density of bubbles. In general, increasing the number of finer particles, produces more bubbles that are physically smaller. It has also been highlighted that finer particles tend to sieve through the coarse particles during rotational molding, and melt first against the wall of the mold.
5. Extensive polymer grinding trials showed that the size and shape of the powder, was controlled by the grinding parameters. Larger powder particles were produced by increasing the clearance between the grinding wheels or reducing the number of teeth on the grinding wheels. Low temperature grinding was shown to produce particles with tails that are more susceptible to producing bubbles.
6. One method used by the rotational molding industry to remove bubbles and pores is to overheat the product. This method was shown to be successful, but had a detrimental effect on the mechanical strengths of the product as they are greatly reduced because of thermal degradation. Also, longer cycle times, caused by this method, reduced the efficiency of the process.
7. Pre-drying of carbon black pigmented material, to remove moisture, had no effect on the end product. The molding contained a similar number of bubbles and pores as moldings from black materials that had not been dried.
8. A low viscosity material (MIL 3725, MFI 25 g/10 min) was shown to produce products that contained no bubbles or surface pores when rotationally molded. Even when this material was removed prematurely from the oven (internal air temperature 150°C), it still produced products without bubbles. This early oven removal time represented a 25% reduction in the overall cycle time.
9. The use of different mold materials was shown not to effect the surface porosity of the molded product. This was because the application of release agent reduced the surface tension of the mold material, which in turn reduced the attractive force causing the polymer to wet and spread evenly over the mold surface. When these mold materials were investigated without release agent, then the surface porosity experienced was significantly reduced, however, removing the polymer from the metal proved to be a problem.
10. The application of six different rotational molding grades of release agent were shown to reduce the surface tension of the mold and hence produce products with similar levels of surface porosity.

11. The use of a thermal imaging camera indicated that the reason why some molds may produce moldings with regions containing no surface pores is because of "hot spots" on the mold, or areas of the mold that are more thermally conductive. The polymer adjacent to these "hot spots" will be subjected to a higher temperature, which will aid the diffusion of air, trapped in the bubble, through the melt.

#### ACKNOWLEDGMENTS

The authors are grateful to the Science and Engineering Research Council, Lin Pac Rotational Moulders, and Neste Chemicals (now Borealis) for the financial support of this work. The work benefitted greatly by the regular inputs from the staff at the sponsoring companies and from Dr. Bob Pittillo of the Polymer Engineering Group. The authors are also indebted to Dr. Jovita Oliveira and Dr. Jose Corvas from the Universidade de Mirho, Portugal, for assistance with the bubble analysis and measurement of melt rheology at low shear rates. Thanks are also due to Dr. Steve Holding from Rapra Technology for determining the molecular weight distributions of various materials.

#### REFERENCES

1. J. L. Throne, *Plastic Process Engineering*, Marcel Dekker Inc., New York.
2. D. Tomo, *Rotational Molding of Polyethylene Powders*, Gordon and Breach, New York (1971).
3. H. R. Howard, "Variables in Rotomolding That are Controllable by the Molder," Association of Rotational Molders (October 1977).
4. R. J. Crawford, *Progress in Rubber and Plastic Technology*, **6**, 1-29 (1991).
5. R. J. Crawford and P. J. Nugent, *Plastics and Rubber Processing and Application*, **17**, 23 (1992).
6. "Symposium on Rotational Molding," USI Chemicals Co, Chicago (November 1965).
7. A. L. McKenna, "The Properties and Economics of Rotationally Moulded Polyethylene," *Progressive Plastics* (December 1965).
8. "Symposium II on Rotational Molding With Linear Powdered Polyethylene," USI Chemicals Co, Chicago (June 1966).
9. M. A. Rao and J. L. Throne, *Polym. Eng. Sci.*, **12**, 237 (1972).
10. D. J. Ramazzotti, "Rotational Molding—The State of the Art," The Society of Plastics Engineers, Regional Technical Conference (October 1975).
11. J. A. Smith, "Perfecting Rotational Molding Techniques for Polycarbonate," Association of Rotational Molder, Conference, Texas (1981).
12. W. E. Foster, *Plast. Technol.*, November 1970, p. 47.
13. J. M. Conway, *Mod. Plast.*, July 1973, p. 64.
14. S. R. Paquette, "A Guide for Selecting Rotational Molding Powders," Society of Plastics Engineers, Regional Technical Conference, p. 13 (March 1969).
15. Anon., *Modern Plastics International*, December 1977, p. 74.
16. G. E. Carrow, *Plastics Design and Processing*, February 1974, p. 19.
17. G. E. Carrow, *Polyolefins II*, p. 177ff., Society of Plastics Engineers (February 1978).
18. J. J. Brenzinch, K. D. Cavender, and G. V. Olhort, *Plast. Technol.*, October 1973, p. 75.
19. E. M. A. Harkin-Jones, PhD thesis, Queen's University of Belfast (1992).
20. M. A. Rao and J. L. Throne, *SPE ANTEC Tech. Papers*, **18**, 759 (1972).
21. R. C. Progelhof, G. Cellier, and J. Throne, *SPE ANTEC Tech. Papers*, **28**, 627 (1982).
22. P. Y. Kelly, "A Microscopic Examination of Rotomoulded Polyethylene," DuPont Canada Incorporation.
23. J. Frenkel, *J. Phys. (USSR)*, **9**, 385 (1945).
24. G. C. Kuczynski and J. Zaplatynsk, *Amer. Ceram. Soc.*, **39**, 349 (1956).
25. G. C. Kuczynski, B. Neuville, and H. P. Toner, *J. Appl. Polym. Sci.*, **14**, 2069 (1970).
26. J. F. Lontz, "Sintering of Polymer Materials," Ch. 1 in *Fundamental Phenomena in the Material Sciences*, L. J. Bonis and H. H. Hanser, Plenum Press, New York (1964).
27. R. J. Crawford and J. A. Scott, *Plast. Rubb. Proc. Appl.*, **7**, 85 (1987).
28. J. A. Scott, PhD thesis, Queen's University of Belfast (1986).
29. R. J. Crawford and L. Xu, *Mater. Sci.*, **28**, 2067 (1993).
30. M. Nelkon and P. Parker, *Advanced Level Physics*, Heinemann Educational Books, London (1977).
31. J. A. Brydson, *Plastics Materials*, Butterworths, London (1989).
32. N. S. Allen, *Degradation and Stabilisation of Polyolefins*, Applied Science Publishers, London (1983).
33. W. Schnabel, *Polymer Degradation—Principles and Practical Applications*, Hanser International, Munich (1981).
34. H. A. Barnes, J. F. Hutton, and K. Walters, *An Introduction to Rheology*, Elsevier, Oxford, U.K. (1989).
35. R. E. Duncan and A. B. Zimmerman, "Rotational Molding of High Density Polyethylene Powders," Society of Plastics Engineers, Regional Technical Conference, p. 50 (March 1969).
36. F. N. Cogswell, *Plastics and Polymers*, February 1973, p. 39.
37. J. Titus, *Engineering Design Handbook: Rotational Molding of Plastic Powder*, Dept of Army Headquarters, United States Army Material Command, AMC Pamphlet, No: 706-312 (April 1975).
38. R. J. Heath, *Prog. Rubb. Plast. Technol.*, **6**, 369 (1990).
39. *Metals Handbook*, 9th Edition, American Society for Metals, Metals Park, Ohio (1985).
40. U. R. Evans, *Corrosion and Oxidation of Metals*, Edward Arnold Ltd., London (1960).